International Journal of Applied Earth Observation and Geoinformation 44 (2016) 159–170

Contents lists available at ScienceDirect

International Journal of Applied Earth Observation and Geoinformation

journal homepage: www.elsevier.com/locate/jag

Multiscale object-based drought monitoring and comparison in rainfed and irrigated agriculture from Landsat 8 OLI imagery

Emre Ozelkan[a,b,c,*], Gang Chen[b,c], Burak Berk Ustundag[a]

[a] Agricultural & Environmental Informatics Research and Application Centre, Istanbul Technical University, 34,469 Maslak, Istanbul, Turkey
[b] Department of Geography and Earth Sciences, University of North Carolina at Charlotte, 9201 University City Blvd, Charlotte, NC 28223, USA
[c] Laboratory for Remote Sensing and Environmental Change (LRSEC), University of North Carolina at Charlotte, 9201 University City Blvd, Charlotte, NC 28223, USA

ARTICLE INFO

Article history:
Received 9 July 2015
Received in revised form 3 August 2015
Accepted 10 August 2015

Keywords:
Drought
Agriculture
SPI
NDVI
Irrigated
Rainfed
GEOBIA
Landsat OLI

ABSTRACT

Drought is a rapidly rising environmental issue that can cause hardly repaired or unrepaired damages to the nature and socio-economy. This is especially true for a region that features arid/semi-arid climate, including the Turkey's most important agricultural district — Southeast Anatolia. In this area, we examined the uncertainties of applying Landsat 8 Operational Land Imager (OLI) NDVI data to estimate meteorological drought – Standardized Precipitation Index (SPI) — measured from 31 in-situ agro-meteorological monitoring stations during spring and summer of 2013 and 2014. Our analysis was designed to address two important, yet under-examined questions: (i) how does the co-existence of rainfed and irrigated agriculture affect remote sensing drought monitoring in an arid/semi-arid region? (ii) What is the role of spatial scale in drought monitoring using a GEOBIA (geographic object-based image analysis) framework? Results show that spatial scale exerted a higher impact on drought monitoring especially in the drier year 2013, during which small scales were found to outperform large scales in general. In addition, consideration of irrigated and rainfed areas separately ensured a better performance in drought analysis. Compared to the positive correlations between SPI and NDVI over the rainfed areas, negative correlations were determined over the irrigated agricultural areas. Finally, the time lag effect was evident in the study, i.e., strong correlations between spring SPI and summer NDVI in both 2013 and 2014. This reflects the fact that spring watering is crucial for the growth and yield of the major crops (i.e., winter wheat, barley and lentil) cultivated in the region.

1. Introduction

Drought is an environmental disaster typically defined as an unusual deficiency in water supply for an extended period (Mishra and Singh, 2010; Vyas et al., 2015). Due to the accelerated climate change, global drought events have dramatically increased in recent years (Mu et al., 2013). It is likely that those events will have a more detrimental impact on the regions that were arid or semi-arid, for example the southeast Anatolia of Turkey (Sensoy, 2003; Sensoy et al., 2008b; Tayanç et al., 2009). Bordered by Syria to the south and Iraq to the southeast, the southeast Anatolia of Turkey has been historically dominated by intensive agricultural practices. According to Turkey's Ministry of Development, the total area of the region is 7.5 million hectares where 3.2 million hectares (11.4% of Turkey's agriculture area) are suitable for agriculture with the rest being covered by pasturelands, shrubberies and forests (Turkish Ministry of Development, 2015). The region's agricultural products for export account for almost 6% of the entire export market of Turkey (Turkish Ministry of Development, 2015). More than half of its population is involved in cultivation related activities (Genc, 2003). However, the employment in agriculture has been consistently decreasing by 8% over the last decade mainly caused by the strengthened drought in the region, which has significantly affected the productivity of crops (Turkish Statistical Institute, 2015). Officially declared by the Government of Turkey, one of the most destructive effects of drought over the southeast Anatolia has been seen since 2008, reducing crop yield by 28% and increasing the national consumer price index inflation rate by almost 2% compared to previous years (Turkish Ministry of Economy, 2015a,b; Union of Turkish Agricultural Chambers, 2015; Turkish Statistical Institute, 2015).

* Corresponding author. Fax: +90 212 285 7501.
E-mail address: emreozelkan@itu.edu.tr (E. Ozelkan).

http://dx.doi.org/10.1016/j.jag.2015.08.003
0303-2434/

Large-scale projects, such as the Southeastern Anatolian Project (GAP) and the Agricultural Monitoring and Information System (TARBIL), have been in progress to mitigate the impact of drought and desertification on the loss in agriculture while maximizing regional socio-economic benefits (Yuksel, 2012; Yurekli, 2015; TARBIL, 2015). Especially for TARBIL, one of the emphases was to establish a large network of in-situ meteorological stations in both rainfed (i.e., farming practices solely relying on rainfall for water) and irrigated agricultural lands, with a goal to understand the fine-scale impact of microclimate on crop yield. And since 2013, such network has successfully covered the southeast Anatolia of Turkey, where our study area was located.

Monitoring meteorological drought and assessing its impact on crops are essential for effective agricultural management (e.g., crop monitoring, yield estimation, and economic planning). Traditionally, such objective is achieved by directly using meteorological drought indices, e.g., the Standardized Precipitation Index (SPI) (McKee et al., 1993), which are computed from the in-situ observation data (e.g., precipitation) collected at a limited number of meteorological stations (Caccamo et al., 2011, Ji and Peters 2003). While those indices are accurate, they lack the ability to provide spatially-explicit drought estimates mainly due to the geographic and economic constraints when establishing in-situ stations (Ozelkan et al., 2014). As a viable solution, remote sensing can provide a wall-to-wall drought estimation by linking field-measured drought indices (e.g., SPI) with a variety of spectral indices, such as Normalized Difference Vegetation Index (NDVI) (Tucker, 1979), Simple Ratio Index (SR) (Tucker, 1979), Vegetation Condition Index (VCI) (Kogan and Sullivan, 1993), Temperature Condition Index (TCI) (Kogan, 1995), Normalized Difference Water Index (NDWI) (Gao, 1996), and Normalized Difference Drought Index (NDDI) (Gu et al., 2007).

Among these indices, NDVI has proven itself a relatively accurate and consistent representation of vegetation vigor, percentage green cover, live biomass, and canopy photosynthetic activity (Tucker, 1979; Ji and Peters, 2003; Anyamba and Tucker, 2005; Rulinda et al., 2012; Mu et al., 2013; Gopinath et al., 2015). The hypothesis for a robust SPI-NDVI relationship over agricultural lands is that the lack of precipitation often leads to vegetation stress or even mortality, with crops exhibiting decreased near-infrared reflectance and increased red reflectance (Ji and Peters, 2003; Caccamo et al., 2011; Wang et al., 2015). Accordingly, NDVI decreases within the range (0, 1). However, the uneven development of agricultural infrastructure (e.g., availability of water suppliers or irrigation systems) and complex microclimates (e.g., spatially varying meteorological parameters such as precipitation, temperature and others) are observed in many regions of the world (Çelik and Gülersoy, 2013; Dadaser-Celik et al., 2008; Ozelkan et al., 2015). This is also true in the southeast Anatolia of Turkey, where both rainfed and irrigated lands co-exist. The uncertainty of remote sensing drought monitoring is possibly introduced by human irrigation practices. While difficult to predict, the frequency of irrigation is often correlated with the severity and length of drought events (Dadaser-Celik et al., 2008). Remote sensing observations over irrigated crops may reflect meteorological drought to some extent, although their relationship is likely to be different from that obtained in rainfed lands. Scientists have also reported that the response of vegetation to drought may exhibit a time lag effect, because drought is a gradual process altering soil moisture (Wang et al., 2003; Gao et al., 2008; Dhakar et al., 2013; Nichol and Abbas, 2015). Similarly, irrigation during one growing season has the potential to significantly affect crop growth and yields in the succeeding seasons (Greene and Kirkham, 1980; Dadaser-Celik et al., 2008; Salmon et al., 2015). Using remote sensing to estimate drought in a region covered by both rainfed and irrigated lands may cause unexpected errors without considering those crucial yet well-studied effects.

While climate is typically considered as a large-scale phenomenon, there has been an increasing need for understanding how small-scale crop lands are influenced by microclimate in precision agriculture (Mbow et al., 2014). The best spatial scale at which SPI and NDVI are correlated can vary across the area of interest attributing to the changing topography and land cover (Briner et al., 2012). Traditionally, image pixels acquired from satellite sensors (e.g., Landsat) are directly used in drought monitoring (Ghulam et al., 2007; Nichol and Abbas, 2015). Some researchers further employed square kernels/windows (e.g., 3-by-3 or 5-by-5 pixels) to take into consideration of the neighborhood characteristics (Caccamo et al., 2011; Ozelkan et al., 2015). However, such practices neglect the fact that the natural environment is not appropriate to be arbitrarily divided into small grids of the same size and shape (Blaschke et al., 2014). Geographic object-based image analysis (GEOBIA) appears to be an ideal solution to address such challenge, because it can extract meaningful geographic objects of varying sizes and shapes and apply these internally homogenous objects as the basic study units in drought monitoring (Chen et al., 2012). GEOBIA further facilitates an investigation of the best spatial scales to achieve desired model accuracy through its unique multiscale analysis (Addink et al., 2007; Chen et al., 2011).

Based upon the above considerations, in this research we used the southeast Anatolia of Turkey as the case study area to address two important, but still under-examined questions: (i) how does the co-existence of rainfed and irrigated agriculture affect remote sensing drought monitoring in an arid/semi-arid region? (ii) What is the role of spatial scale in drought monitoring using a GEOBIA framework?

2. Data and Methodology

2.1. Study Area

The study area is located in the heart of the southeastern Anatolia of Turkey between 37°15′–39°37′ eastern meridians and 36°38′–37°56′ northern parallels, north of the Turkey–Syria border covering an area of 36,500 km^2 (Fig. 1). The elevation of the area ranges from 2667 m in the northwest to 67 m in the southeast with variable geographic and microclimatic conditions. Generally, the region's climate is named southeastern Anatolia continental climate, featuring hot and dry summer with air temperature above 30 °C, and mild spring and autumn with extreme temperature anomalies occurring more frequently over the last decade (Sensoy, 2003; Sensoy et al., 2008a). The area's long-term annual average temperature is 16.4 °C, and its annual average precipitation is 565.8 mm that varies through space and time between 350 and 800 mm (Sensoy, 2003; Sensoy et al., 2008a). The annual relative humidity is averaged at 53.6%. Such low humidity increases evaporation that strengthens the drought in summer especially when the precipitation is very low (Sensoy, 2003; Sensoy et al., 2008a). Consequently, the southeastern Anatolia is often considered as the driest region in Turkey (Sensoy, 2003; Sensoy et al., 2008a).

According to the current climatic conditions, there are two agricultural growing seasons per year, i.e., early season (autumn–summer) and late season (spring–autumn) (Alganci et al., 2014; GAP Regional Development Administration, 2015). Winter wheat and barley are the major crops in the study area, typically cultivated in the early season (Alganci et al., 2014; GAP Regional Development Administration, 2015). The general agricultural practices for wheat and barley have four stages: (i) tillage, seeding and fertilization in autumn; (ii) pest control, weeding and fertilization between winter and the beginning of spring; (iii) irrigation in spring; and (iv) harvesting in summer (GAP Regional Development Administration, 2015). The third major crop of the region is lentil

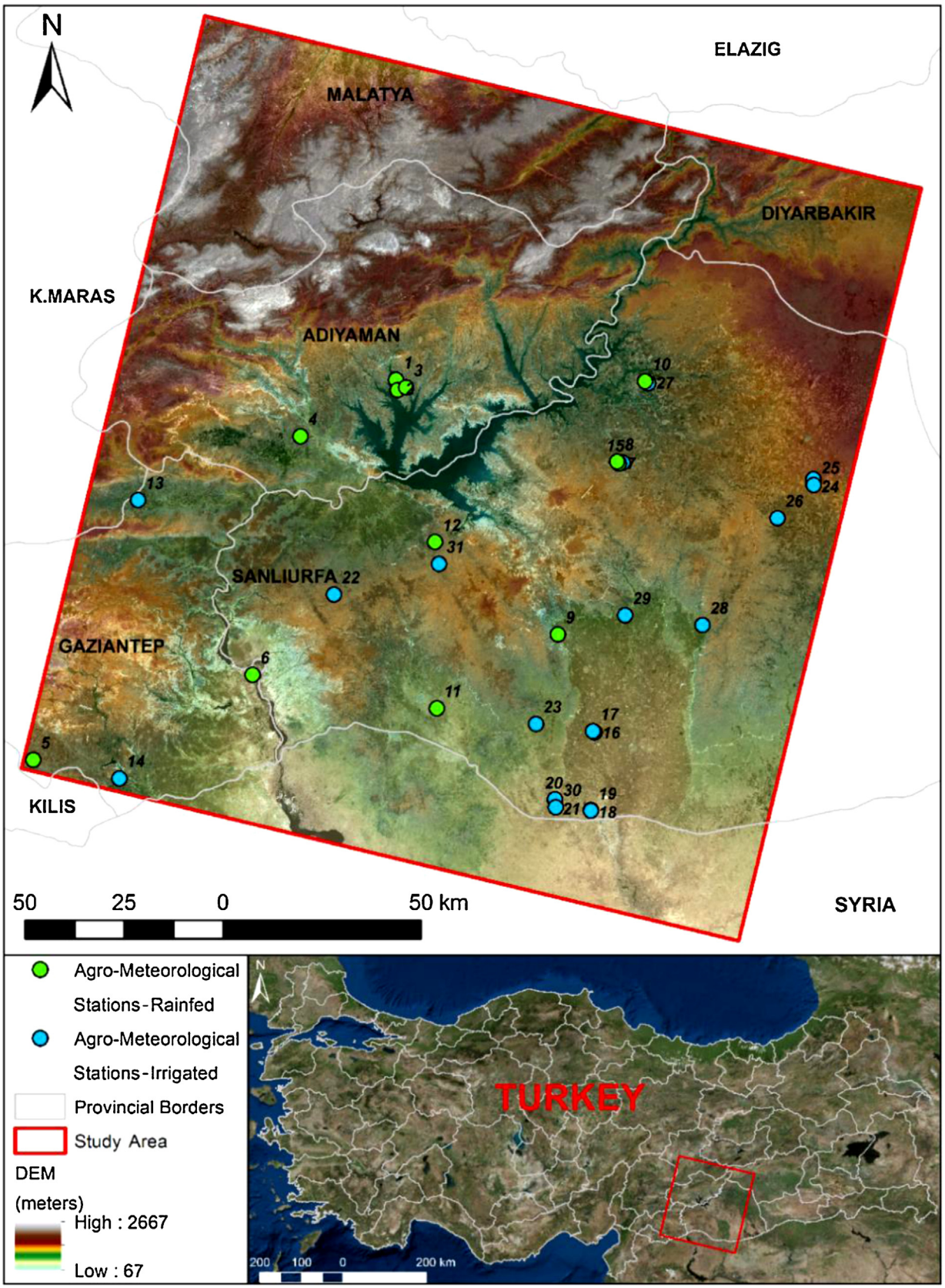

Fig. 1. Study area and agro-meteorological stations with Digital Elevation Model (DEM) and a Landsat 8 Operational Land Imager (OLI) true color image as backdrop.

Table 1
Drought classes and corresponding SPI values (Caccamo et al., 2011).

Drought Class	Range of SPI Value
Extremely wet	>2.00
Severely wet	1.5 to 1.99
Moderately wet	1.0 to 1.49
Mildly wet	0.99 to 0
Mild drought	0 to -0.99
Moderate drought	−1 to −1.49
Severe drought	−1.5 to −1.99
Extreme drought	<−2.00

that has similar growing stages as winter wheat and barley, except that irrigation is not conducted because of its nature of high tolerance to drought. For this study, we emphasized on spring and summer seasons, based on the considerations that both seasons are the crucial periods for the development of wheat and barley, and their phenological variation can be well captured using remote sensing.

2.2. Field data and pre-processing

Field data from 31 agro-meteorological monitoring stations were acquired for two years of 2013 and 2014, as part of a new large-scale agricultural management initiative TARBIL (Fig. 1). The stations comprise almost all types of microclimates over the agricultural fields in the study area (TARBIL, 2015). Records of each station include crop type, irrigation status (i.e., rainfed versus irrigated), and precipitation. The irrigation status was used to classify the stations into rainfed (12 stations) and irrigated agriculture (19 stations). Compared to previous studies, one of the most important advantages of this study is that all the stations are within the agricultural areas directly reflecting drought and irrigation conditions.

A widely-used probability index, SPI (Standardized Precipitation Index) was calculated to represent meteorological drought as follows:

$$\mathrm{SPI_i} = \frac{X_\mathrm{i} - X_\mathrm{mean}}{\sigma} \quad (1)$$

where X_i is the precipitation of an investigated (i) period, and X_mean and σ are the long-term mean and standard deviation of the measured precipitation, respectively (McKee et al., 1993; Dhakar et al., 2013). Note that long term data was obtained from the closest and geographically similar climate stations of Turkish State Meteorological Service. SPI ranges from 2.00 and above (extremely wet) to −2.00 and less (extremely dry) with mild conditions ranging from 0.99 to −0.99 (Table 1) (Caccamo et al., 2011). Compared to other in-situ drought measurements, SPI has several advantages such as simplicity, statistical consistency, robustness, dimensionality, and temporal flexibility (Dhakar et al., 2013; Du et al., 2013). Here, we calculated 3-month SPI values for the purpose of assessing the seasonal variation of drought. Fig. 2 shows all the stations' SPI values for the spring and summer of 2013 and 2014. The average SPI values of the spring in 2013 and 2014 were −1.33 and −1.33 (moderate drought) with standard deviation of 0.76 and 0.71, respectively. The average SPI values of the summer were −0.21 (mild drought) and 0.43 (mild wet) with standard deviation of 0.25 and 0.64, respectively. The variation of SPI amongst the monitoring stations reflects variable microclimatic conditions in the study area.

2.3. Remote sensing data and pre-processing

The study area coincided with the extent of one Landsat image scene (path/row: 173/34). A total of 13 Landsat 8 Operational Land Imager (OLI) images over the area were downloaded from the USGS data portal (USGS, 2014). To ensure a proper representation of the seasons we studied, the images were acquired monthly from spring

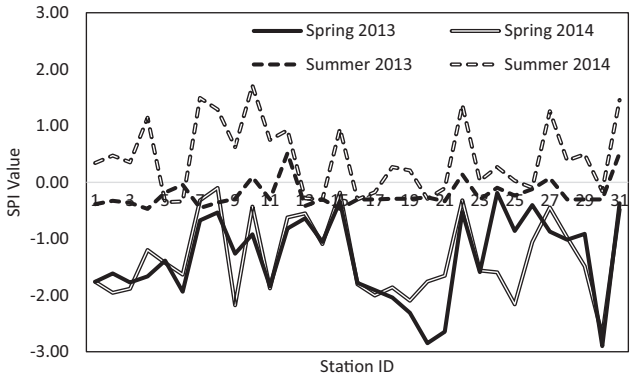

Fig. 2. Seasonal average SPI values measured from 31 agro-meteorological monitoring stations.

and summer of 2013 and 2014. All the images were atmospherically and geometrically corrected by the vendor, with pixel values representing surface reflectance. NDVI was calculated as follows (Tucker, 1979):

$$\mathrm{NDVI} = \frac{(\lambda_\mathrm{NIR} + \lambda_\mathrm{RED})}{(\lambda_\mathrm{NIR} - \lambda_\mathrm{RED})} \quad (2)$$

where λ_RED and λ_NIR are the reflectance at the red and near infrared spectral ranges, respectively. As a classic vegetation index, NDVI correlates well with vegetation photosynthetic activity, primary productivity, water stress, and drought response (Tucker, 1979). NDVI of vegetation often has values more than 0.2, and it increases towards 1.0 in the areas covered by healthy and abundant plants with high leaf water content. In this study, NDVI was calculated for each Landsat image scene and then aggregated into two seasons of two years, i.e., spring 2013, summer 2013, spring 2014, summer 2014 (Fig. 3).

2.4. Data analysis

The relationship between remote sensing NDVI imagery and in-situ SPI data was analyzed in two major steps: (i) generating multiple spatial scales using GEOBIA segmentation, and (ii) assessing the relationship between NDVI and SPI in rainfed versus irrigated agriculture using statistical analysis. Specifically,

(i) Each of the four NDVI images was segmented to derive image-objects, i.e., homogenous pixel clusters of varying sizes and shapes (Blaschke and Hay, 2001). However, such homogeneity is a relative concept. An image-object may represent a small cluster of plants or a large patch of agricultural land. Hence, a total of 12 spatial scales (a representation of 12 mean object sizes) were extracted from the small pixel level of 0.0009 $\mathrm{km^2}$ to the large object level of 1.0396 $\mathrm{km^2}$ (a simulation of the 1 km spatial resolution MODIS data). Fig. 4 shows the corresponding scale parameters from 0 to 220 used in eCognition Developer 8 (Trimble Navigation, Sunnyvale, California). For the purpose of consistency, the same set of parameters (shape: 0.1, and compactness: 0.5) were employed in segmentation at each scale (Chen et al., 2014). Finally, all the NDVI pixel values were aggregated within objects.
(ii) Because the 31 agro-meteorological monitoring stations were separately located in rainfed (12 stations) and irrigated lands (19 stations), the Pearson's correlation coefficients (r) between NDVI and SPI were calculated and compared for three categories, including the rainfed, the irrigated, and the combined without distinguishing irrigation policy. For each category, we analyzed the NDVI-SPI relationship at all the 12 spatial scales.

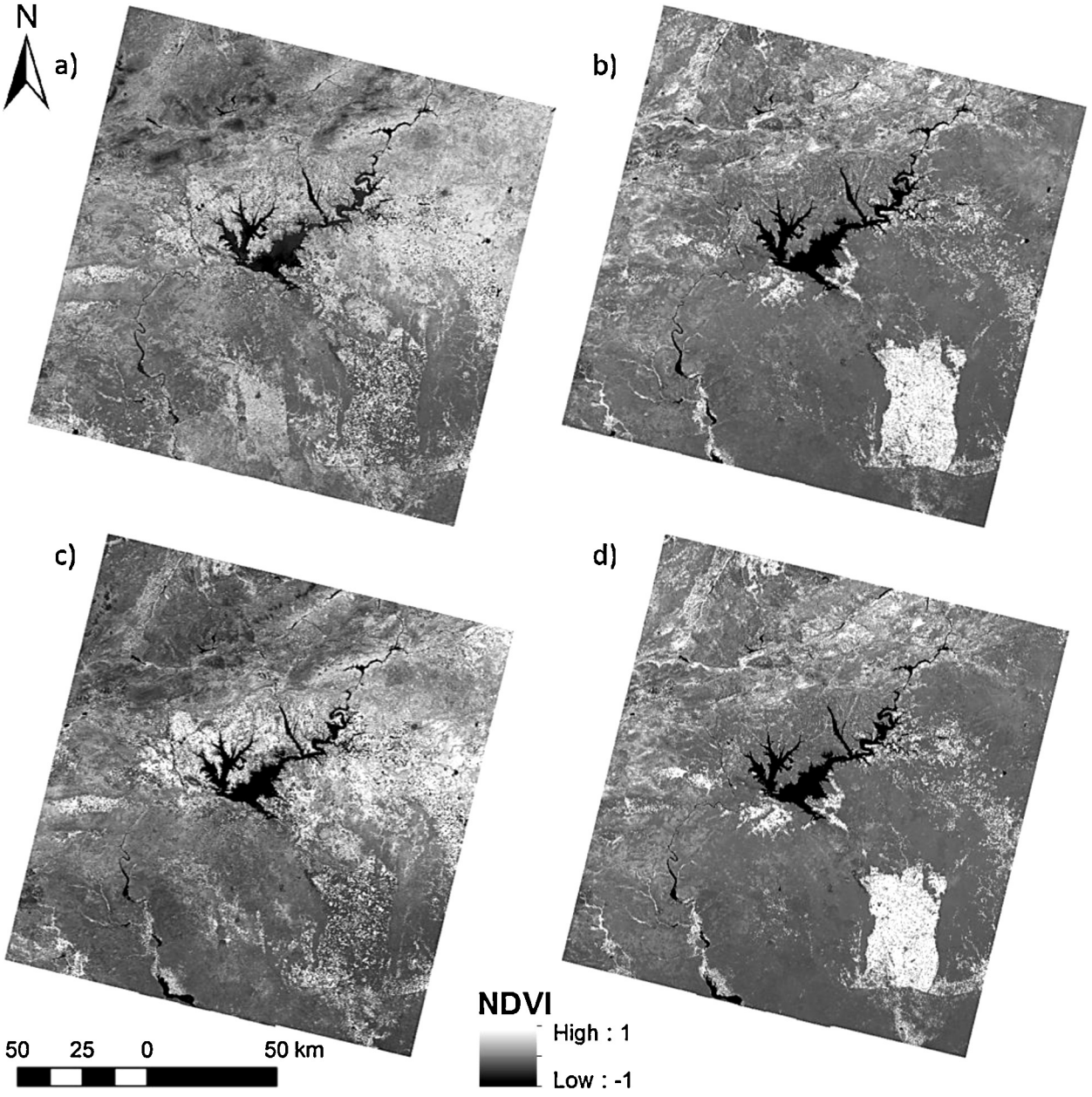

Fig. 3. NDVI images calculated for (a) spring 2013, (b) summer 2013, (c) spring 2014, and (d) summer 2014.

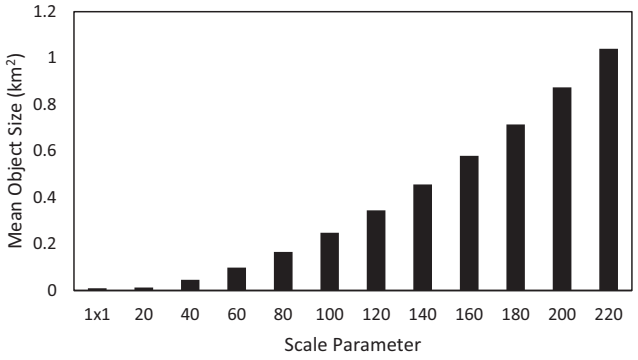

Fig. 4. The relationship between scale parameter (used in eCognition) and mean object size. 1×1 represents the pixel-level analysis.

To understand the time lag effect, we not only compared NDVI and SPI of the same season in spring and summer, but also correlated spring SPI with summer NDVI of the same year, with the purpose to analyze whether drought and irrigation have a long-term impact on crop growth and health. In all cases, we also calculated and reported the significance F (SF), which is a significance probability of ANOVA (Analysis of Variance).

3. Results and discussion

3.1. Impact of spatial scale on drought monitoring

Spatial scale was discovered to have varying impacts on the relationship between SPI and NDVI. Specifically, for the year of 2013, smaller scales were likely to have a more positive impact on the SPI-NDVI correlation for the rainfed, the irrigated and all the areas combined (Figs. 5 and 6). With the increase of scale, their correlations decreased for all the three types of agricultural

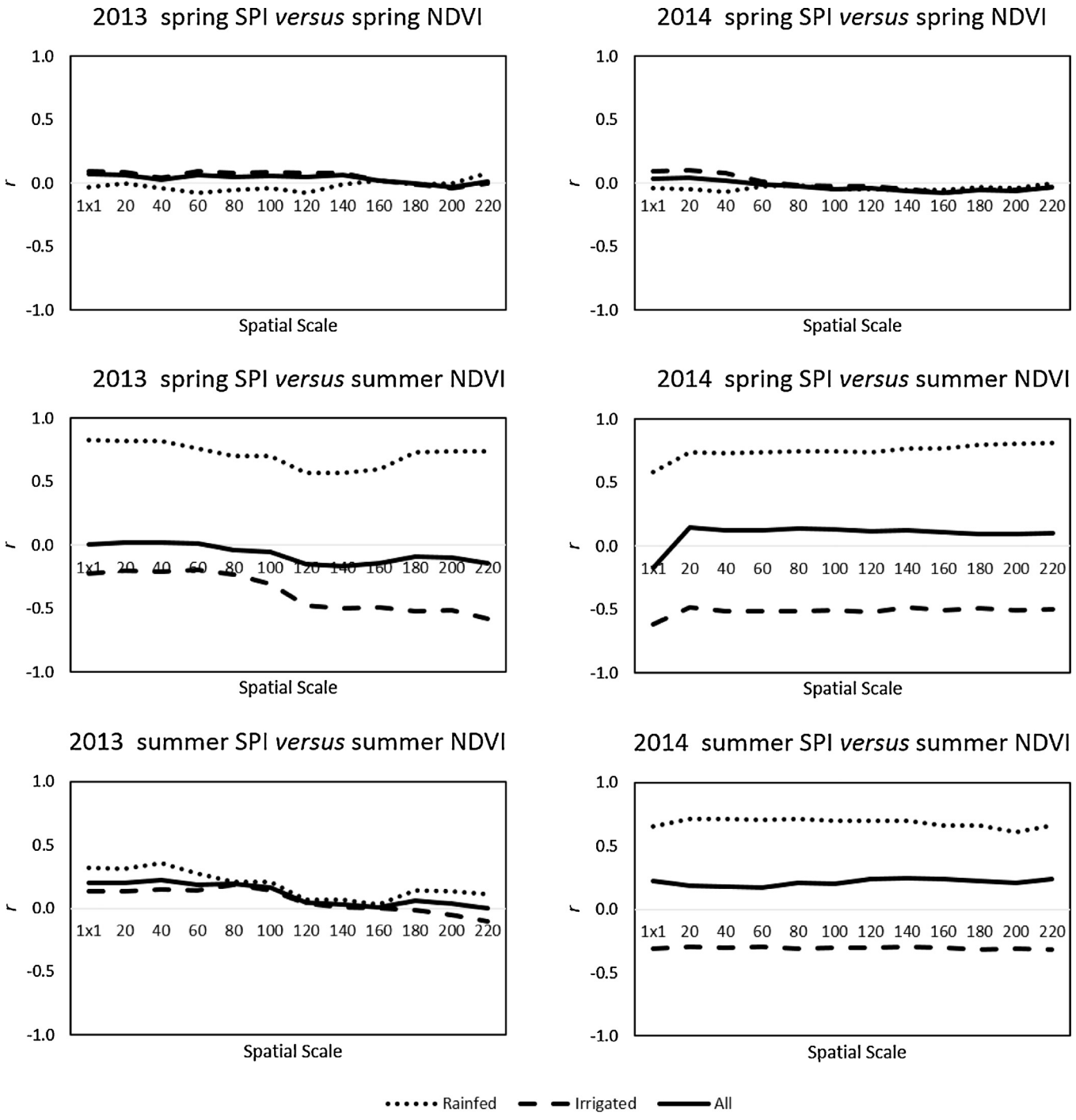

Fig. 5. The distribution of Pearson's correlation coefficient (r) values between SPI and NDVI across spatial scales for the rainfed, the irrigated and all the areas combined.

land classification. One exception occurred in the spring SPI versus summer NDVI of 2013, during which the correlations were increasing with the increasing scales for irrigated and combined areas. In spring SPI versus spring NDVI, the correlations were already weak ($-0.1 < r < 0.1$) and scale was not able to show a noticeable impact. In contrast, spatial scale was found to have minimized influence over the relationship between SPI and NDVI in all the seasonal comparisons for the rainfed, the irrigated and all the areas combined (Figs. 5 and 6). Because 2013 was drier than 2014 (Fig. 2), it is possible that the lack of precipitation in 2013 may have introduced high spatial variation in features of agriculture areas such as soil moisture, crop vigor and canopy (Ji and Peters, 2003; Gopinath et al., in press). Consequently, small scales performed slightly better than large scales in capturing such variation in general (Figs. 5 and 6). However, when rainfall was relatively abundant in 2014, soil may have had a higher homogeneity in water content. Microclimate and local topography did not unveil a significant impact on crop health and growth.

3.2. Same-season SPI-NDVI correlation over rainfed, irrigated and all areas

Generally, no significant relationship was discovered between spring SPI and spring NDVI for any of the three irrigation sta-

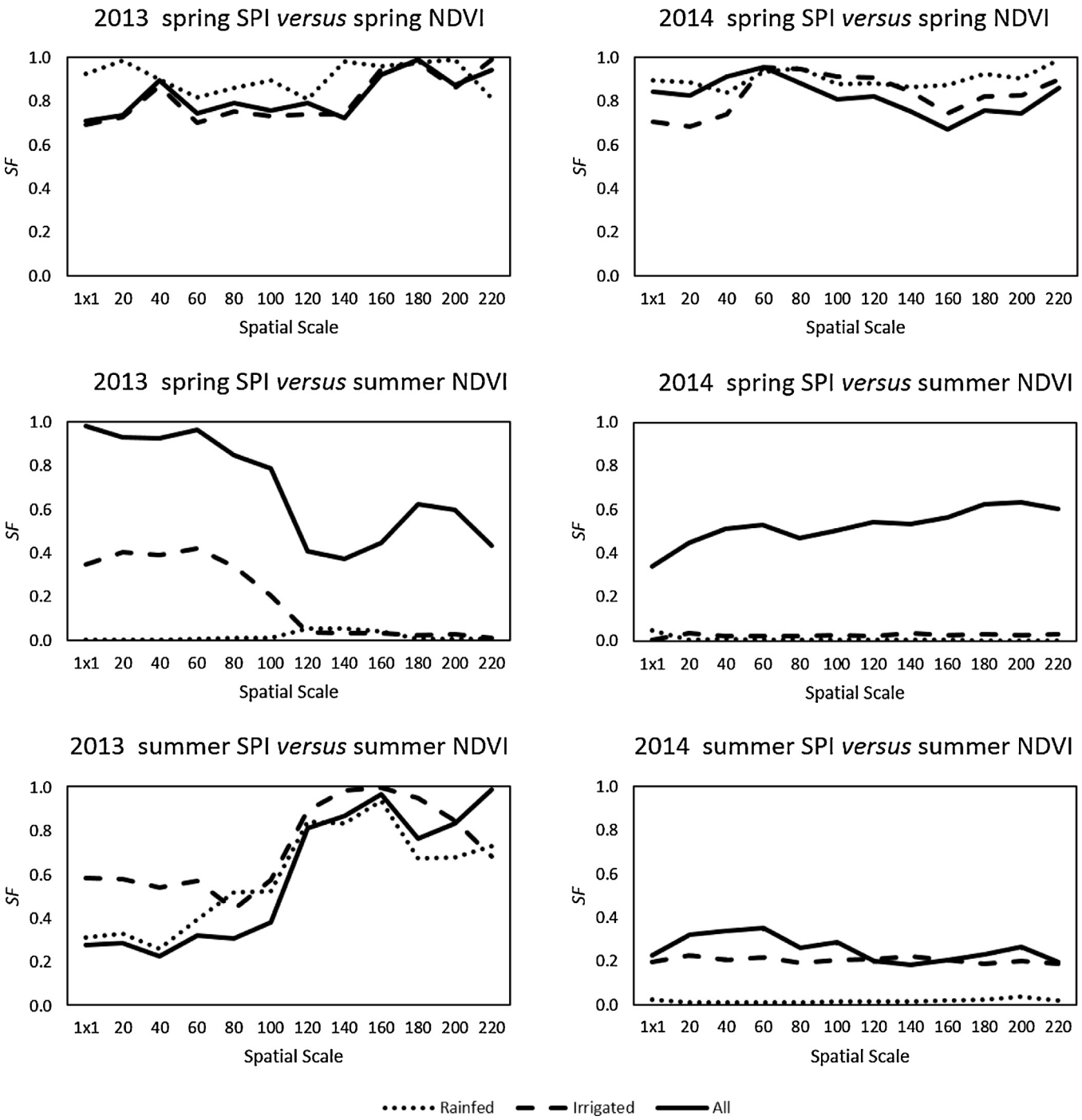

Fig. 6. The distribution of significance *F* (*SF*) values between SPI and NDVI across spatial scales for the rainfed, the irrigated and all the areas combined.

tuses, i.e., the rainfed, the irrigated and all the areas combined (Figs. 5 and 6). Even for the best result, the SPI-NDVI correlation was found to be close to 0, with *SF* over 0.67 (Fig. 7). However, the summer SPI values were found to better correlate with summer NDVI (Figs. 5 and 6). Specifically, the correlations in the rainfed lands were positive and superior to those obtained from the irrigated lands. The results for the combined lands without distinguishing irrigation types were found in the middle. This suggests that irrigation did have a negative impact on remote sensing drought mapping by introducing uncertainties and errors. The findings are consistent with several previous studies of the similar topic (Dhakar et al., 2013; Ezzine et al., 2014).

We further noticed that the correlation between SPI and NDVI was even negative in summer 2014 over irrigated areas (Figs. 5, 7 and 8). It is possible that irrigation practices were reinforced in the areas with relative water deficit leading a negative correlation. Because such correlation was weak, it may be also caused by the complex local environment and microclimate. In either case, we suggest that fine-scale drought monitoring should take into the consideration of the difference in irrigation policy. To improve the accuracy of remote sensing based drought monitoring, it is imperative that irrigated and rainfed agricultural lands are separately modelled and analyzed. Hence, a prerequisite step may

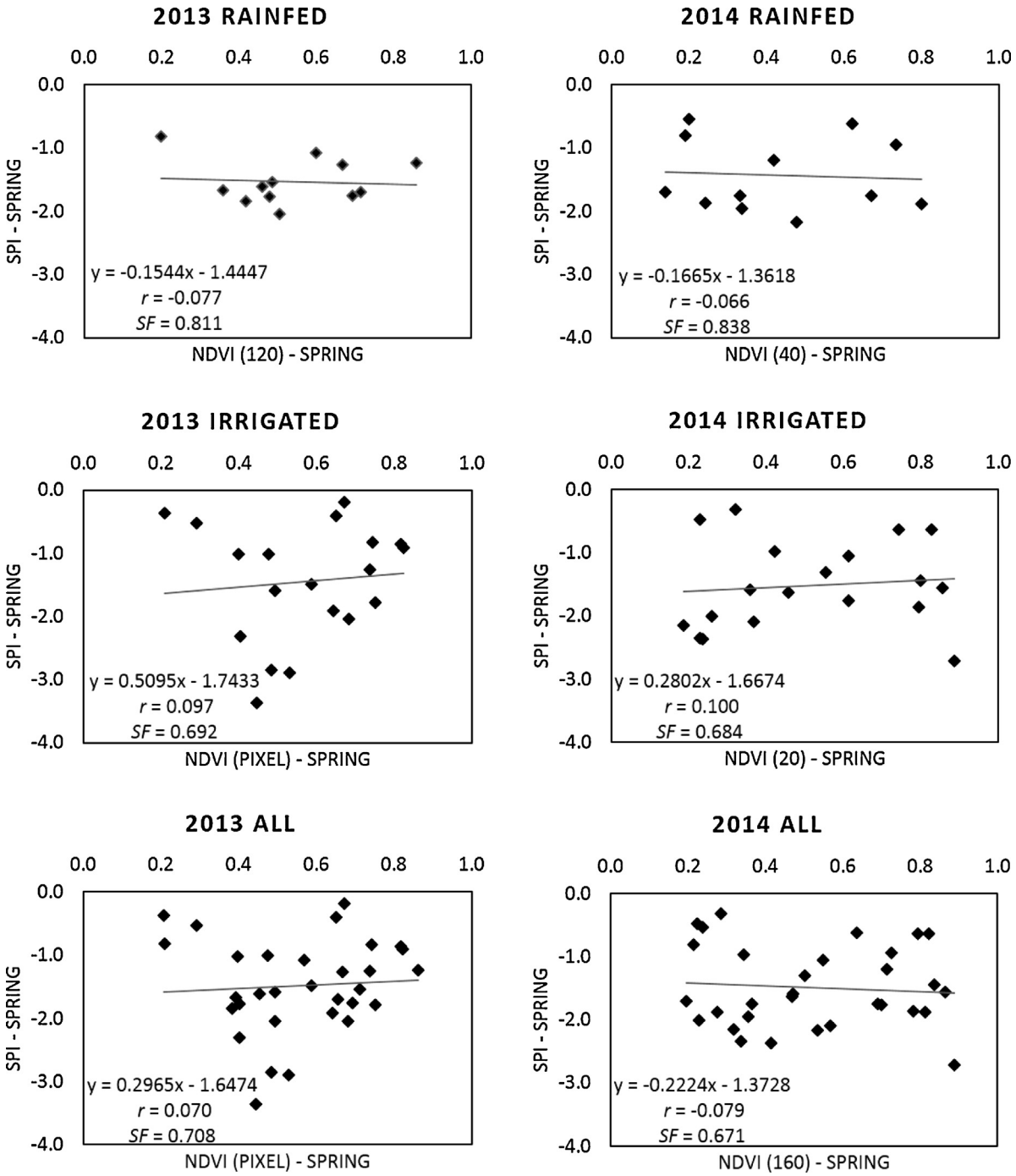

Fig. 7. The best correlations between spring SPI and spring NDVI of 2013 and 2014 for the rainfed, the irrigated and all the areas combined.

involve an accurate mapping of these two types of agriculture, if the local irrigation policy was not known.

3.3. Evaluation of time lag effect

Our results revealed a noticeable time lag effect for both years of 2013 and 2014. For year 2013, the best correlations between spring SPI and summer NDVI were 0.829 ($SF = 0.001$) and −0.580 ($SF = 0.009$) for the rainfed and irrigated lands, respectively (Fig. 9). Similarly, for 2014 the correlations were 0.806 ($SF = 0.002$) and −0.622 ($SF = 0.004$) for the rainfed and irrigated lands, respectively (Fig. 9). This finding is compatible with the phenological development of the major crops (wheat and barley) cultivated in our study area, because they need sufficient water in spring more than the other seasons to ensure a healthy growth (Greene and Kirkham, 1980; Ozkan and Akcaoz 2002; Dadaser-Celik et al., 2008). More specifically, in an arid or semi-arid region, crop growth and yield could vary prominently from year to year attributing to high variation in precipitation (Morell et al., 2011). For many crop types, even if rainfall or irrigation occurred in one growing season (e.g., during spring flowering and ripening), crop yields in the harvesting season could be significantly higher than those without early season rainfall or irrigation (Greene and Kirkham, 1980; Dadaser-Celik et al., 2008; Morell et al., 2011; Amossé et al., 2013; Salmon

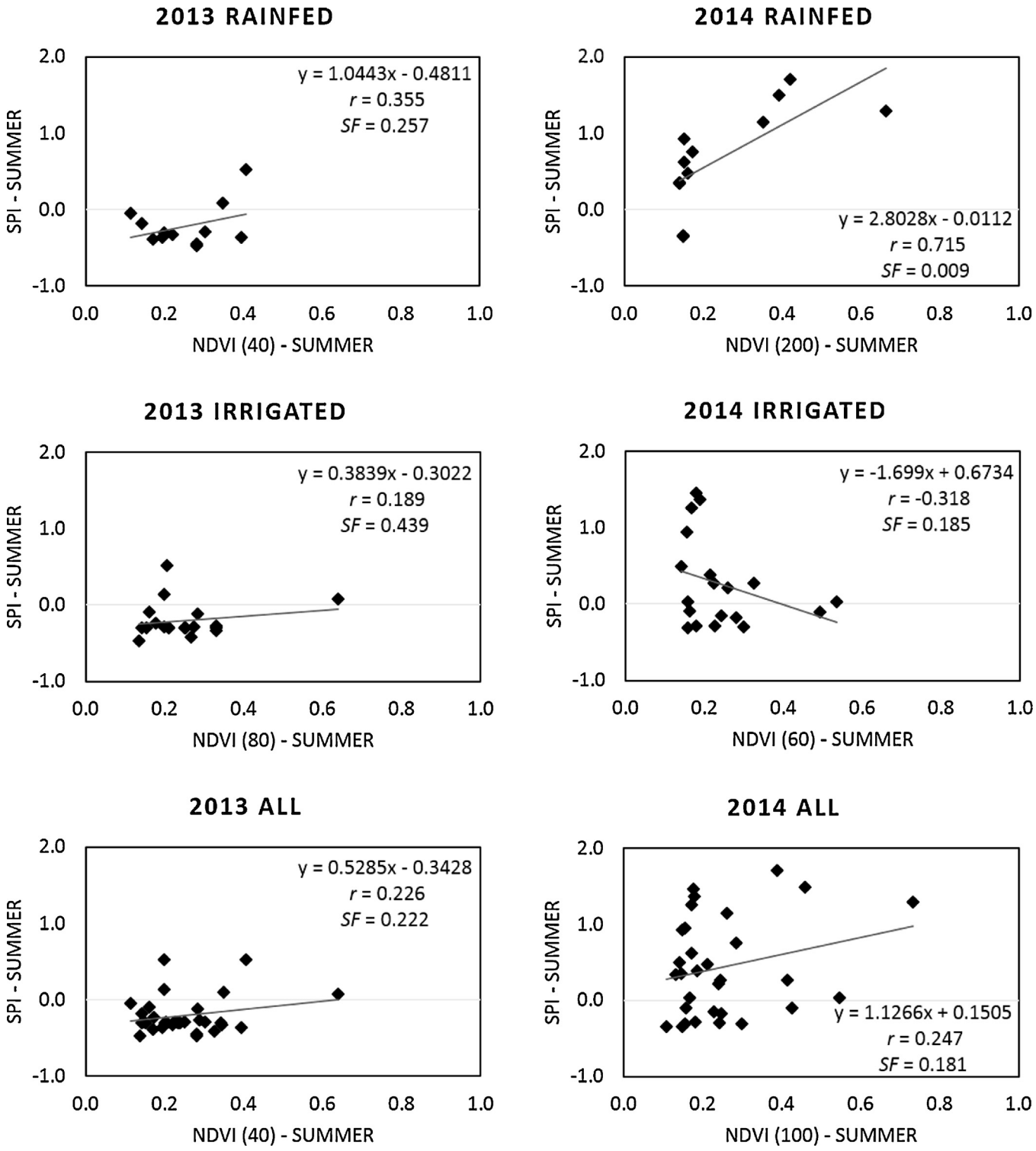

Fig. 8. The best correlations between summer SPI and summer NDVI of 2013 and 2014 for the rainfed, the irrigated and all the areas combined.

et al., 2015). This may explain the relatively strong correlations between spring SPI and summer NDVI. Compared to the positive correlation over the lands watered by natural rainfall (i.e., rainfed areas), a negative SPI-NDVI correlation was discovered in the agricultural lands benefiting from human irrigation (i.e., irrigated areas). Finally, the correlations considering the time lag effect were found stronger than those using remote sensing to estimate meteorological drought of the same/present season.

4. Conclusions

This study analyzed the uncertainties of applying Landsat 8 OLI imagery to estimate meteorological drought in the heart of the Southeast Anatolia of Turkey, an arid/semi-arid region experiencing strengthened drought over the past decade. We evaluated the impact of season (spring versus summer), and spatial scale (12 scales from small pixel level of 0.0009 km^2 to large stand level

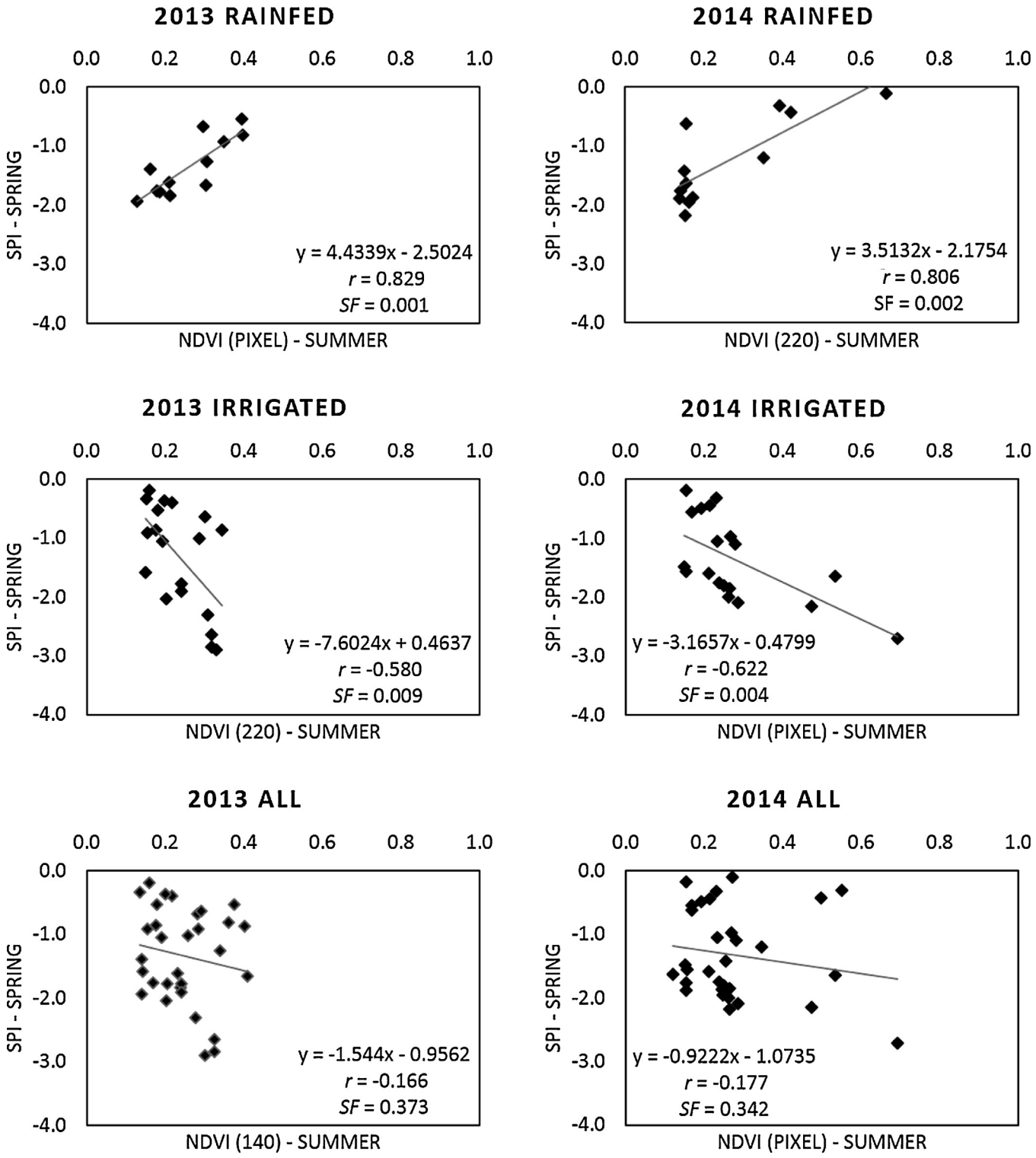

Fig. 9. The best correlations between spring SPI and summer NDVI of 2013 and 2014 for the rainfed, the irrigated and all the areas combined.

of 1.0396 km^2) on the SPI-NDVI relationship in rainfed and irrigated agricultural lands, respectively. Results include three main points:

a) In an arid/semi-arid region, spatial scale may exert a high impact on remote sensing drought monitoring especially in a dry season/year, during which small scales were found to outperform large scales in general.
b) Irrigated and rainfed areas should be separated in drought monitoring to ensure a better performance in remote sensing modeling. Compared to the positive correlations between SPI and NDVI over the rainfed areas, negative correlations were discovered over the irrigated agricultural areas.
c) The time lag effect was evident in our study area. The best correlations were obtained between spring SPI and summer NDVI, reflecting the crucial influence of spring watering on crop growth

and summer yield in the region. Such relationship was even strong and significant for the irrigated lands.

As one of the major developing countries, Turkey has a significant agriculture sector that is crucial for the nation's economic development. Remote sensing can be of great benefits for the areas (especially the arid and semi-arid) facing severe drought and desertification. These regions, e.g., Southeast Anatolia – the driest area of Turkey, often feature small-scale uneven development of agriculture infrastructure. Spatially-explicit and accurate drought mapping can assist in consistent and effective farmland management, reducing the chance to cause serious problems such as waterlogging, salinization, and decrease in yield (Mukhtarov et al., 2014).

Acknowledgment

The authors would like to thank the Turkish Agricultural Monitoring and Information System Project (TARBIL) for field data acquisition and funding support. Gang Chen gratefully acknowledges the support from the University of North Carolina at Charlotte through Junior Faculty Development Award.

References

Addink, E.A., de Jong, S.M., Pebesma, E.J., 2007. The importance of scale in object-based mapping of vegetation parameters with hyperspectral imagery. Photogramm. Eng. Remote Sens. 73, 905–912, http://dx.doi.org/10.14358/PERS.73.8.905.

Alganci, U., Ozdogan, M., Sertel, E., Ormeci, C., 2014. Estimating maize and cotton yield in southeastern Turkey with integrated use of satellite images, meteorological data and digital photographs. Field Crops Res. 157, 8–19, http://dx.doi.org/10.1016/j.fcr.2013.12.006.

Amossé, C., Jeuffroy, M., David, C., 2013. Relay intercropping of legume cover crops in organic winter wheat: effects on performance and resource availability. Field Crops Res. 145, 78–87, http://dx.doi.org/10.1016/j.fcr.2013.02.010.

Anyamba, A., Tucker, C.J., 2005. Analysis of Sahelian vegetation dynamics using NOAA-AVHRR NDVI data from 1981 to 2003. J. Arid Environ. 63, 1847–1859, http://dx.doi.org/10.1016/j.jaridenv.2005.03.007.

Blaschke, T., Hay, G.J., 2001. Object-oriented image analysis and scale-space: theory and methods for modeling and evaluating multiscale landscape structure. Int. Arch. Photogramm. Remote Sens. 34, 22–29.

Blaschke, T., Hay, G.J., Kelly, M., Lang, S., Hofmann, P., Addink, E., Feitosa, R.Q., van der Meer, F., van der Werff, H., van Coillie, F., Tiede, D., 2014. Geographic object-based image analysis -towards a new paradigm. ISPRS J. Photogramm. Remote Sens. 87, 180–191, http://dx.doi.org/10.1016/j.isprsjprs.2013.09.014.

Briner, S., Elkin, C., Huber, R., Grêt-Regamey, A., 2012. Assessing the impacts of economic and climate changes on land-use in mountain regions: a spatial dynamic modeling approach. Agric. Ecosyst. Environ. 149, 50–63, http://dx.doi.org/10.1016/j.agee.2011.12.011.

Caccamo, G., Chisholm, L.A., Bradstock, R.A., Puotinen, M.L., 2011. Assessing the sensitivity of MODIS to monitor drought in high biomass ecosystems. Remote Sens. Environ. 115 (10), 2626–2639, http://dx.doi.org/10.1016/j.rse.2011.05.018.

Chen, G., Hay, G.J., Carvalho, L.M.T., Wulder, M.A., 2012. Object-based change detection. Int. J. Remote Sens. 33 (14), 4434–4457, http://dx.doi.org/10.1080/01431161.2011.648285.

Chen, G., Hay, G.J., Castilla, G., St-Onge, B., 2011. A multiscale geographic object-based image analysis to estimate lidar- measured forest canopy height using Quickbird imagery. Int. J. Geogr. Inform. Sci. 25 (6), 877–893, http://dx.doi.org/10.1080/13658816.2010.496729.

Chen, G., Zhao, K., Powers, R., 2014. Assessment of the image misregistration effects on object-based change detection. ISPRS J. Photogramm. Remote Sens. 87, 19–27, http://dx.doi.org/10.1016/j.isprsjprs.2013.10.007.

Çelik, M.A., Gülersoy, A.E., 2013. An examination of the effects of Southeastern Anatolia Project (GAP) on agricultural patterns changes using remote sensing. J. Int. Soc. Res. 6 (28), 46–54.

Dadaser-Celik, F., Brezonik, P.L., Stefan, H.G., 2008. Agricultural and environmental changes after irrigation management transfer in the Develi Basin, Turkey. Irrig. Drain. Syst. 22, 47–66, http://dx.doi.org/10.1007/s10795-007-9032-4.

Dhakar, R., Sehgal, V.K., Pradhan, S., 2013. Study on inter-seasonal and intra-seasonal relationships of meteorological and agricultural drought indices in the Rajasthan State of India. J. Arid Environ. 97, 108–119, http://dx.doi.org/10.1016/j.jaridenv.2013.06.001.

Du, L., Tian, Q., Yu, T., Meng, Q., Jancso, T., Udvardy, P., Huang, Y., 2013. A comprehensive drought monitoring method integrating MODIS and TRMM data. Int. J Appl. Earth Observ. Geoinform. 23, 245–253, http://dx.doi.org/10.1016/j.jag.2012.09.010.

Ezzine, H., Bouziane, A., Ouazar, D., 2014. Seasonal comparisons of meteorological and agricultural drought indices in Morocco using open short time-series data. Int. J. Appl. Earth Observ. Geoinform. 26, 36–48, http://dx.doi.org/10.1016/j.jag.2013.05.005.

Gao, B.C., 1996. NDWI—a normalized difference water index for remote sensing of vegetation liquid water from space. Remote Sens. Environ. 58, 257–266, http://dx.doi.org/10.1016/S0034-4257(96)67-3.

Gao, M., Qin, Z., Zhang, H., Lu, L., Zhou, X., Yang, X., 2008. Remote sensing of agro-droughts in Guangdong Province of China using MODIS satellite data. Sensors 8, 4687–4708, http://dx.doi.org/10.3390/s8084687.

GAP Regional Development Administration, May 2015. GAP - Agricultural Education and Informing Project – GAP Region Agriculture Calendar (in Turkish: GAP Bolgesi Tarim Takvimi), <http://www.gapteyap.org/category/sanliurfa/>.

Genc, O., 2003. Southeast Anatolia region economic and social condition report (in Turkish: Guneydogu Anadolu bolgesi ekonomik ve sosyal durum raporu). Development Bank of Turkey, <http://www.kalkinma.com.tr/data/file/raporlar/esa/ga/2003-ga/ga-03-04-05_gab.pdf/>.

Ghulam, A., Qin, Q., Teyip, T., Li, Z., 2007. Modified perpendicular drought index (MPDI): a real-time drought monitoring method. ISPRS J. Photogramm. Remote Sens. 62 (2), 150–164, http://dx.doi.org/10.1016/j.isprsjprs.2007.03.002.

Gopinath, G., Ambili, G.K., Gregory, S.J., Anusha, C.K., 2015. Drought risk mapping of south-western state in the Indian peninsula —a web based application. J. Environ. Manage., http://dx.doi.org/10.1016/j.jenvman.2014.12.040, in press.

Greene, D.M., Kirkham, M.B., 1980. Water-conserving wheat irrigation schedules based on climatic records. Irrig. Sci. 1 (4), 241–246, http://dx.doi.org/10.1007/BF00277629.

Gu, Y., Brown, J.F., Verdin, J.P., Wardlow, B., 2007. A five-year analysis of MODIS NDVI and NDWI for grassland drought assessment over the central Great Plains of the United States. Geophys. Res. Lett. 34, L06407, http://dx.doi.org/10.1029/2006GL029127.

Ji, L., Peters, A.J., 2003. Assessing vegetation response to drought in the northern Great Plains using vegetation and drought indices. Remote Sens. Environ. 87 (1), 85–98, http://dx.doi.org/10.1016/S0034-4257(03)174-3.

Kogan, F.N., Sullivan, J., 1993. Development of global drought-watch system using NOAA/AVHRR data. Adv. Space Res. 13 (5), 219–222, http://dx.doi.org/10.1016/0273-1177(93)90548-P.

Kogan, F.N., 1995. Application of vegetation index and brightness temperature for drought detection. Adv. Space Res. 15 (11), 91–100, http://dx.doi.org/10.1016/0273-1177(95)79-T.

Mbow, C., Smith, P., Skole, D., Duguma, L., Bustamante, M., 2014. Achieving mitigation and adaptation to climate change through sustainable agroforestry practices in Africa. Curr. Opin. Environ. Sustain. 6, 8–14, http://dx.doi.org/10.1016/j.cosust.2013.09.002.

McKee, T.B., Doesken, N.J., Kleist, J., 1993. The relationship of drought frequency and duration to time scales. Proceedings of Eighth Conference on Applied Climatology, Anaheim, CA. American Meteorological Society, Boston, MA, 179–184.

Morell, F.J., Lampurlanés, J., Álvaro-Fuentes, J., Cantero-Martínez, C., 2011. Yield and water use efficiency of barley in a semiarid Mediterranean agroecosystem: long-term effects of tillage and N fertilization. Soil Tillage Res. 117, 76–84, http://dx.doi.org/10.1016/j.still.2011.09.002.

Mishra, A.K., Singh, V.P., 2010. A review of drought concepts. J. Hydrol. 391 (1-2), 202–216, http://dx.doi.org/10.1016/j.jhydrol.2010.07.012.

Mu, Q., Zhao, M., Kimball, J.S., McDowell, N.G., Running, S.W., 2013. A remotely sensed global terrestrial drought severity index. Bull. Amer. Meteor. Soc. 94, 83–98, http://dx.doi.org/10.1175/BAMS-D-11-00213.1.

Mukhtarov, F., Fox, S., Mukhamedova, N., Wegerich, K., 2014. Interactive institutional design and contextual relevance: water user groups in Turkey, Azerbaijan and Uzbekistan. Environ. Sci. Policy, http://dx.doi.org/10.1016/j.envsci.2014.10.006, in press.

Nichol, J.E., Abbas, S., 2015. Integration of remote sensing datasets for local scale assessment and prediction of drought. Sci. Total Environ. 505, 503–507, http://dx.doi.org/10.1016/j.scitotenv.2014.09.099.

Ozelkan, E., Bagis, S., Ozelkan, E.C., Ustundag, B.B., Ormeci, C., 2014. Land surface temperature retrieval for climate analysis and association with climate data. Eur. J. Remote Sens. 47, 655–669, http://dx.doi.org/10.5721/EuJRS20144737.

Ozelkan, E., Bagis, S., Ozelkan, E.C., Ustundag, B.B., Yucel, M., Ormeci, C., 2015. Spatial interpolation of climatic variables using land surface temperature and modified inverse distance weighting. Int. J. Remote Sens. 36 (4), 1000–1025, http://dx.doi.org/10.1080/01431161.2015.1007248.

Ozkan, B., Akcaoz, H., 2002. Impacts of climate factors on yields for selected crops in the Southern Turkey. Mitig. Adapt. Strat. Global Change 7 (4), 367–380, http://dx.doi.org/10.1023/A.1024792318063.

Rulinda, C.M., Dilo, A., Bijker, W., Stein, A., 2012. Characterising and quantifying vegetative drought in East Africa using fuzzy modelling and NDVI data. J. Arid Environ. 78, 169–178, http://dx.doi.org/10.1016/j.jaridenv.2011.11.016.

Salmon, J.M., Friedl, M.A., Frolking, S., Wisser, D., Douglas, E.M., 2015. Global rain-fed, irrigated, and paddy croplands: A new high resolution map derived from remote sensing, crop inventories and climate data. Int. J. Appl. Earth Observ. Geoinform. 38, 321–334, http://dx.doi.org/10.1016/j.jag.2015.01.014.

Sensoy, S., 2003. Turkey Climate Classification (in Turkish: Türkiye İklim Sınıflandırması). Turkish State Meteorological Services Report. <http://www.mgm.gov.tr/files/genel/sss/iklimsiniflandirmalariturkiye.pdf/>.

Sensoy, S., Demircan, M., Ulupinar, Y., Balta, Z., 2008. Climate of Turkey (in Turkish: Türkiye İklimi). Turkish State Meteorological Service Report. <http://www.mgm.gov.tr/files/iklim/turkiye_iklimi.pdf/>.
Sensoy, S., Demircan, M., Ulupinar, Y., Balta, Z., 2008. Climate of Turkey. <http://dmi.gov.tr/files/en-us/climateofturkey.pdf/>.
TARBIL (Agricultural Monitoring and Information System), May 2015. <www.tarbil.com/>.
Tayanç, M., Im, U., Dogruel, M., Karaca, M., 2009. Climate change in Turkey for the last half century. Clim. Change 94, 483–502, http://dx.doi.org/10.1007/s10584-008-9511-0.
Tucker, C.J., 1979. Red and photographic infrared linear combinations for monitoring vegetation. Remote Sens. Environ. 8, 127–150, http://dx.doi.org/10.1016/0034-4257(79)90013-0.
Turkish Ministry of Economy, 2015. Economy Screen. Available online: <http://www.ekonomi.gov.tr/portal/faces/eko/ekonomiInline2/>.
Turkish Statistical Institute, 2015. Statistic Database. Available online: <http://www.turkstat.gov.tr/Start.do/>.
Turkish Ministry of Development, 2015. GAP Region Development Administration, Southeastern Anatolia Project (GAP). Available online: <www.gap.gov.tr>.
Union of Turkish Agricultural Chambers, 2015. In spite of decrease in employment in agriculture sector, unemployement was kept in single-digit (in Turkish: Tarım istihdamı azalmasına rağmen işsizliği tek hanede tuttu). Available online: <http://www.tzob.org.tr/Bas%C4%B1n-Odas%C4%B1/Haberler/ArtMID/470/ArticleID/1391/Tar%C4%B1m-istihdam%C4%B1-azalmas%C4%B1na-ra%C4%9Fmen-i%C5%9Fsizli%C4%9Fi-tek-hanede-tuttu>.
USGS, December 2014. LANDSAT surface reflectance-derived spectral indices. <http://landsat.usgs.gov/documents/si_product_guide.pdf/>.
Wang, J., Rich, P.M., Price, K.P., 2003. Temporal responses of NDVI to precipitation and temperature in the central Great Plains, USA. Int. J. Remote Sens. 24 (11), 2345–2364, http://dx.doi.org/10.1080/01431160210154812.
Wang, H., Chen, A., Wang, Q., He, B., 2015. Drought dynamics and impacts on vegetation in China from 1982 to 2011. Ecol. Eng. 75, 303–307, http://dx.doi.org/10.1016/j.ecoleng.2014.11.063.
Vyas, S.S., Bhattacharya, B.K., Nigam, R., Guhathakurta, P., Ghosh, C., hattopadhyay, N., Gairola, R.M., 2015. A combined deficit index for regional agricultural drought assessment over semi-arid tract of India using geostationary meteorological satellite data. Int. J. Appl. Earth Observ. Geoinform. 39, 28–39, http://dx.doi.org/10.1016/j.jag.2015.02.009.
Yuksel, I., 2012. Water development for hydroelectric in southeastern Anatolia project (GAP) in Turkey. Renew. Energ. 39 (1), 17–23, http://dx.doi.org/10.1016/j.renene.2011.08.006.
Yurekli, K., 2015. Impact of climate variability on precipitation in the Upper Euphrates-Tigris Rivers Basin of Southeast Turkey. Atmos. Res. 154, 25–38, http://dx.doi.org/10.1016/j.atmosres.2014.11.002.